phys. stat. sol. (b) **180**, 357 (1993)

Subject classification: 63.10; 63.20; S5; S5.11

Institut für Theoretische Physik II (Festkörperphysik) der Westfälischen Wilhelms-Universität Münster[1])

Phonon Dispersion Curves of Diamond and Silicon within the Quasi-Ion Model

By

M. MOHAUPT, C. FALTER, M. KLENNER, and W. LUDWIG

The phonon dispersion curves for diamond and silicon in the quasi-ion model are calculated and additionally the effect of anisotropic breathing is studied. Within the rigid quasi-ion model (RIM) the influence on the phonon dispersion of the localization of the expansion set (Gaussians) for the quasi-ions is discussed. Furthermore the phonon dispersion curves are investigated taking anisotropic breathing into account. Such an extension allows to influence special modes in the spectrum, in particular the LA-mode at the L point which is poorly represented in the RIM. Also calculated are phonon-induced changes of the electronic density in this model for some modes. Anisotropic breathing is associated with a quadrupole contribution to the displacement-induced change in density in contrast to the RIM where the quadrupole moment vanishes for symmetry reasons.

Es wird die Phonondispersion von Diamant und Silizium im Quasi-Ionen-Modell berechnet und zusätzlich die Effekte anisotropen Breathings studiert. Im starren Quasi-Ionen-Modell (RIM) wird der Einfluß der Lokalisierung der Entwicklungsfunktionen (Gaußfunktionen) für die Quasi-Ionen auf die Phonondispersion diskutiert. Weiterhin wird die Phonondispersion bei Berücksichtigung von anisotropem Breathing untersucht. Diese Erweiterung erlaubt die Beeinflussung einzelner Moden des Spektrums, z. B. der LA-Mode am L-Punkt, die im RIM nur schlecht wiedergegeben wird. Zusätzlich werden phononeninduzierte (Elektronen)Dichteänderungen in diesem Modell für einige Moden berechnet. Anisotropes Breathing ist dabei mit einem Quadrupolbeitrag zur auslenkungsinduzierten Dichteänderung verbunden, der im RIM aus Symmetriegründen verschwindet.

1. Introduction

Theoretical investigations of phonon spectra in solids within the density response theory require a very high numerical effort. A simpler description is given by the quasi-ion model, where the total density is decomposed into contributions uniquely assigned to single atoms or sublattices [1, 2]. These "partial densities", together with the corresponding ion cores are called quasi-ions. Within this approach the simplest approximation to calculate the phonon dispersion of a crystal then consists in neglecting distortions of the quasi-ions during the vibration. A further simplification is the description of the quasi-ion densities by a set of Gaussians. Distortions are described by special models, where essential contributions are rigid rotations or spherical breathing of the quasi-ions. The two latter distortion models do not influence the frequencies at the Γ point and do not improve the LA(L)-mode significantly. (The effect of the rotations on the latter mode vanishes for symmetry reasons.) Another model with more degrees of freedom is the anisotropic breathing. In this model the localization centers of the Gaussians are considered variable. The

[1]) Wilhelm-Klemm-Str. 10, D-48149 Münster, Federal Republic of Germany.

displacement of an atom leads to specific displacements of the surrounding Gaussians. In practice, however, this idea has to be modified somewhat in order to avoid technical problems.

2. The Quasi-Ion Model

A decomposition of the total electron density into partial densities is possible by consideration of a configuration where the atoms are displaced. The displacement-induced electron density redistribution $\boldsymbol{P}$ describes the change of the electron density ϱ when a atom is displaced [1, 2]

$$\boldsymbol{P}_\alpha^m(\boldsymbol{r}) := \left.\frac{\partial \varrho(\boldsymbol{r})}{\partial \boldsymbol{R}_\alpha^m}\right|_0 . \tag{1}$$

$\boldsymbol{R}_\alpha^m$ denotes the position of the α-th atom in the m-th unit cell of the crystal. We decompose the vector field $\boldsymbol{P}_\alpha^m(\boldsymbol{r})$ into its gradient and rotational parts,

$$\boldsymbol{P}_\alpha^m(\boldsymbol{r}) = -\nabla \varrho_\alpha^m(\boldsymbol{r}) + \nabla \times \boldsymbol{w}_\alpha^m(\boldsymbol{r}) , \tag{2}$$

$$\varrho_\alpha^m(\boldsymbol{r}) = \frac{1}{4\pi} \nabla \cdot \int \mathrm{d}^3 r' \, \frac{\boldsymbol{P}_\alpha^m(\boldsymbol{r}')}{|\boldsymbol{r} - \boldsymbol{r}'|} , \tag{3a}$$

$$\boldsymbol{w}_\alpha^m(\boldsymbol{r}) = \frac{1}{4\pi} \nabla \times \int \mathrm{d}^3 r' \, \frac{\boldsymbol{P}_\alpha^m(\boldsymbol{r}')}{|\boldsymbol{r} - \boldsymbol{r}'|} . \tag{3b}$$

The quantities $\varrho_\alpha^m(\boldsymbol{r})$ are called "quasi-ion" or "partial" densities. The first term in (2) describes a rigid displacement of ϱ_α^m, whereas the second term can be looked upon as describing "distortions" of the quasi-ions due to the displacement.

The total density can be written as a unique superposition of the quasi-ion densities,

$$\varrho(\boldsymbol{r}) = \sum_{m,\alpha} \varrho_\alpha^m(\boldsymbol{r}) =: \sum_{m,\alpha} \varrho_\alpha(\boldsymbol{r} - \boldsymbol{R}_\alpha^m) . \tag{4}$$

In principle, $\boldsymbol{P}_\alpha^m(\boldsymbol{r})$ and hence $\varrho_\alpha^m(\boldsymbol{r})$ can be calculated via the density response function, but in practice the quasi-ion densities are easily determined by fitting to (calculated) total densities and eventually to experimental phonon frequencies.

The quasi-ion densities are approximated by a superposition of Gaussians

$$\varrho_\alpha(\boldsymbol{r}) = \sum_{s=1}^{3} \sum_{\nu=1}^{\nu_s} \sum_{\lambda=1}^{\lambda_s} \left(\frac{\gamma_{\alpha\lambda}^s}{\pi}\right)^{3/2} C_{\alpha\lambda}^s \exp\left[-\gamma_{\alpha\lambda}^s (\boldsymbol{r} - \boldsymbol{R}_{\alpha\lambda}^{s\nu})^2\right] , \tag{5}$$

s denotes the type of localization:

$s = 1$: localization at the center of the atom;

$s = 2$: localization on the bonds;

$s = 3$: localization on the line connecting the next-nearest neighbors.

For a given localization type s, λ numbers the inequivalent Gaussians of this type and ν the localization centers equivalent by symmetry, e.g. the four bonds of an atom in the diamond structure. $\boldsymbol{R}$ are the localization centers, γ the decay constants, and C the amplitudes of the Gaussians.

The parameters are fitted to experimental phonon frequencies from [3, 4] for silicon and [5 to 7] for diamond and to calculated total densities from [8] for diamond and [9] for silicon.

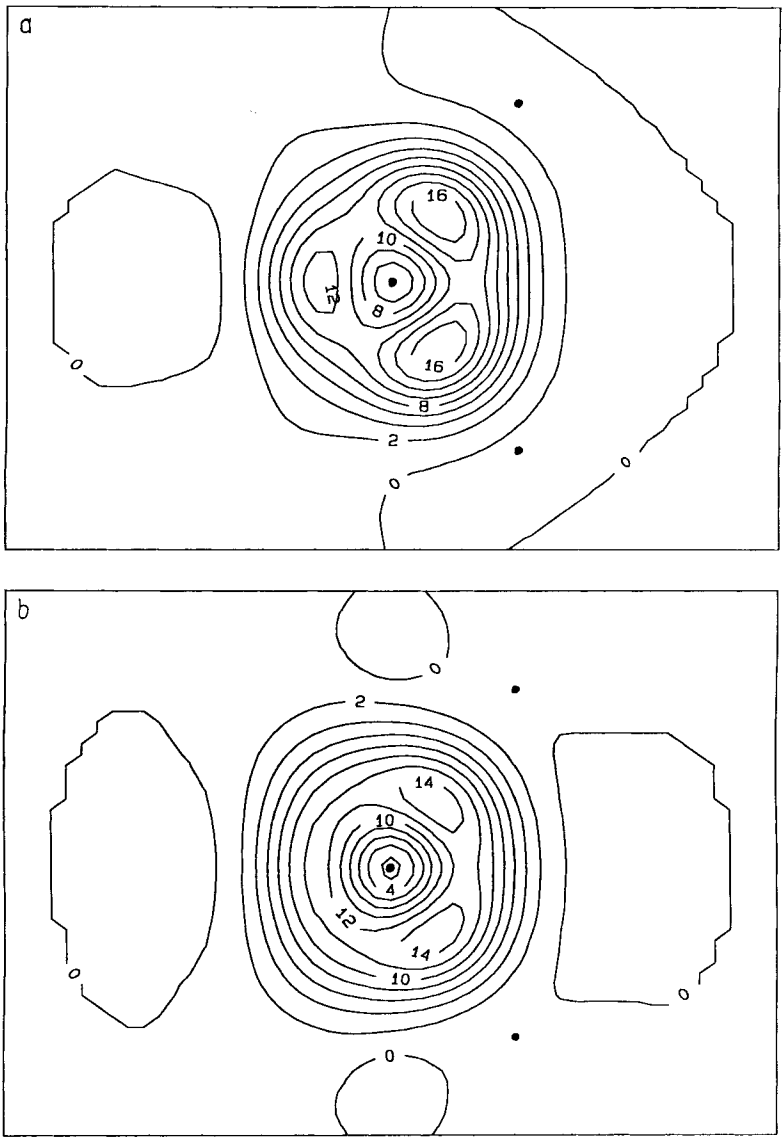

Fig. 1. Contour plot of the quasi-ion density of silicon (In Fig. 1 to 4 the units are electrons per cell.) Atoms are indicated as dots. The plot refers to a $(0, \bar{1}, 1)$ plane. a) $s = 1, 2$; b) $s = 1, 2, 3$ in (5)

Fig. 1 shows the quasi-ion density of silicon with three Gaussians for each type of localization. In Fig. 1a only Gaussians of localization types $s = 1$ and $s = 2$ have been used whereas Gaussians of localization type $s = 3$ have been additionally taken into account in Fig. 1b. The quasi-ion densities of diamond for the same localization types are shown in Fig. 2. The most remarkable feature in both figures is the maximum located at approximately 1/3 of the bond length. The density is more contracted around the ions in case only Gaussians of type $s = 1$ and $s = 2$ taken into account. The corresponding total

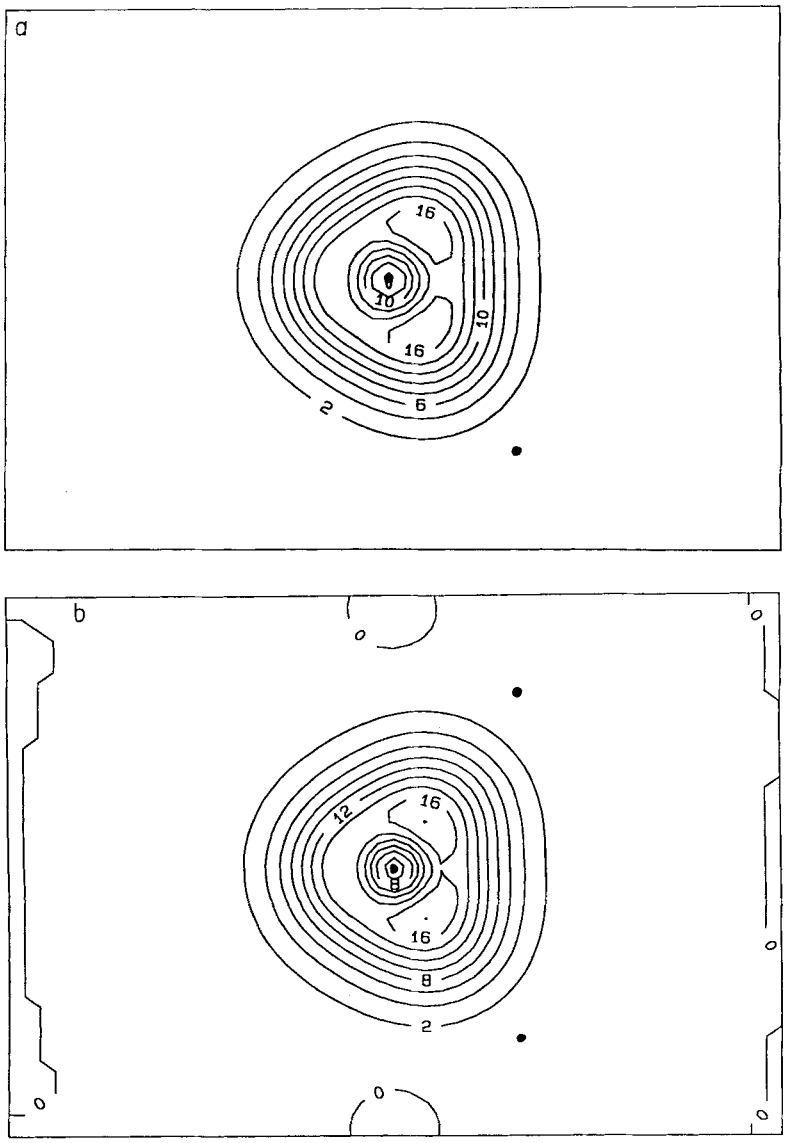

Fig. 2. Contour plot of the quasi-ion density of diamond. Atoms are indicated as dots. The plot refers to a $(0, \bar{1}, 1)$ plane. a) $s = 1, 2$; b) $s = 1, 2, 3$ in (5)

densities are shown in Fig. 3 and 4. Compared to experimental densities for silicon [10, 11] we obtain a better agreement when Gaussians of localization type $s = 3$ are included (Fig. 3b). In the latter case there is an elongation of the density in the middle of the bond, a feature we do not find if only Gaussians of type $s = 1$ and $s = 2$ are used. Diamond shows an analogous behavior. The agreement with [8] is better in the case of Fig. 4b, where the maximum at 1/3 of the bond length is more pronounced.

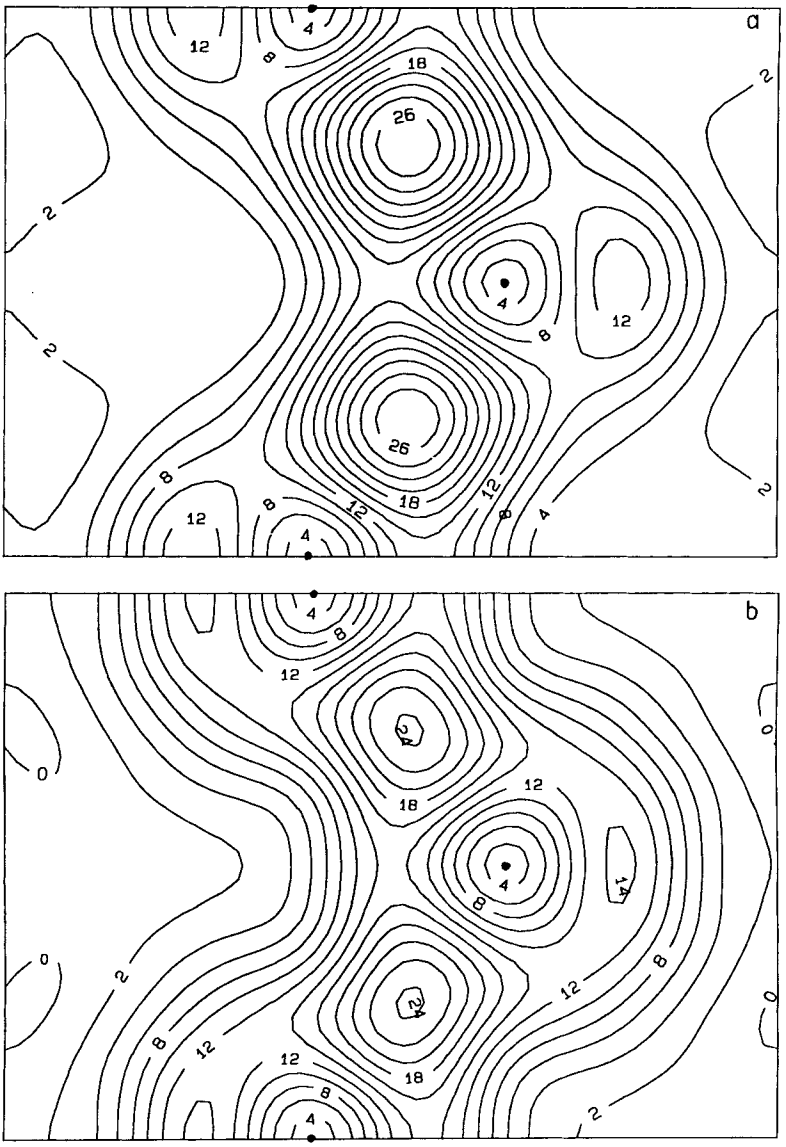

Fig. 3. Contour plot of the total density of silicon. Atoms are indicated as dots. The plot refers to a $(0, \bar{1}, 1)$ plane. a) $s = 1, 2$; b) $s = 1, 2, 3$ in (5)

Taking into account in (2) the gradient part only,

$$\boldsymbol{P}_{\alpha}^{m}(\boldsymbol{r}) \approx -\nabla \varrho_{\alpha}^{m}(\boldsymbol{r}), \tag{6}$$

we obtain the rigid quasi-ion model for $\boldsymbol{P}_{\alpha}^{m}(\boldsymbol{r})$.

The phonon dispersion curves of silicon and diamond within the rigid quasi-ion model are shown in Fig. 5 and 6, respectively. The phonon dispersion in Fig. 5a and 6a corresponds to the quasi-ion density in Fig. 1a and 2a, and the dispersion in Fig. 5b and 6b to the

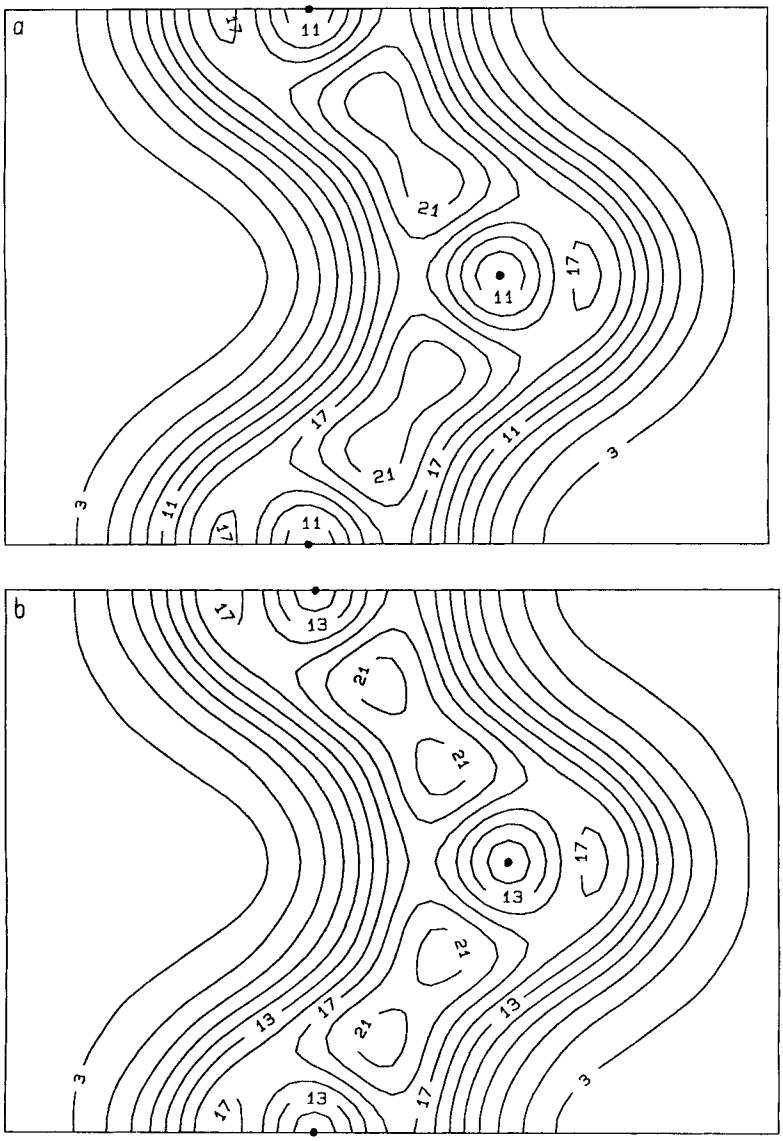

Fig. 4. Contour plot of the total density of diamond. Atoms are indicated as dots. The plot refers to a $(0, \bar{1}, 1)$ plane. a) $s = 1, 2$; b) $s = 1, 2, 3$ in (5)

quasi-ion density in Fig. 1b and 2b, respectively. For the (pseudo-)potential in these calculations a local form of Appelbaum-Hamann type [12] has been used for both materials.

As for the densities, we find a better agreement with the experimental data for both materials if Gaussians of type $s = 3$ are included. In particular, for diamond the agreement with the experimental data is good in the latter case, only the calculated TA(X)-mode is a bit too high. The situation is similar in the case of silicon, but additionally the LA(L)-mode frequency is still too low and the TA(L)-mode still too high. Influencing the TA(X)-mode

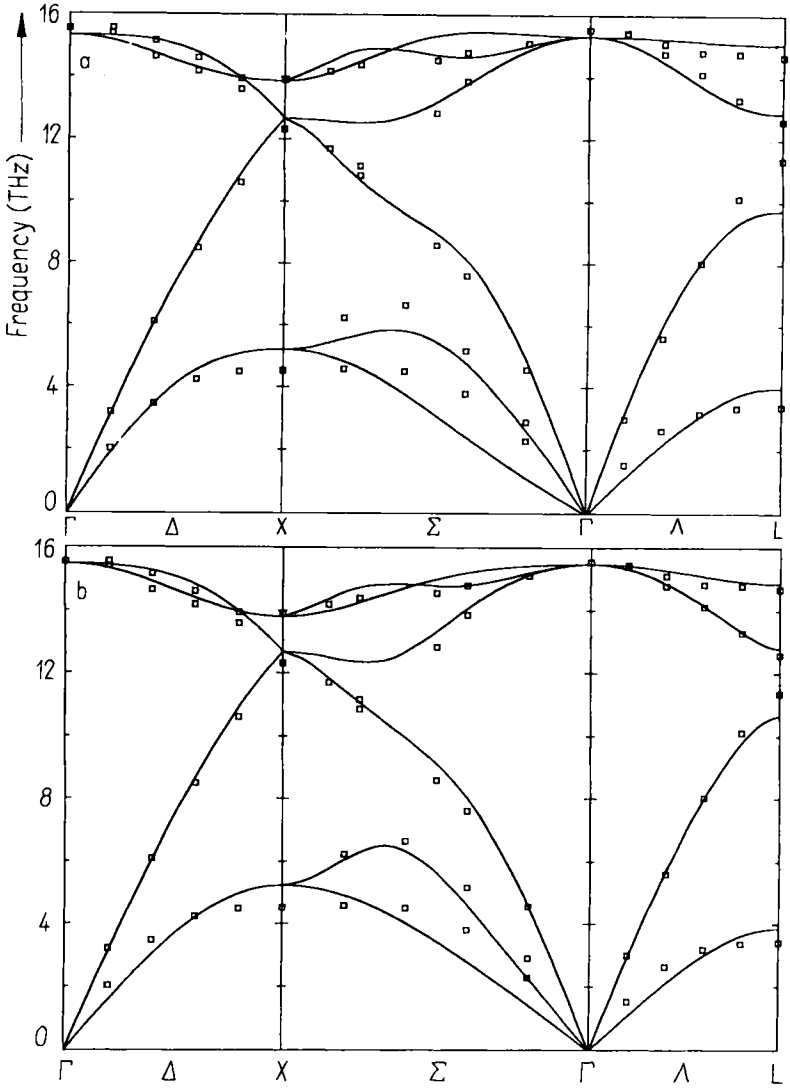

Fig. 5. Calculated phonon dispersion curves of silicon (full lines) within the rigid quasi-ion model in the main symmetry directions $\Delta \approx [1, 0, 0]$, $\Sigma \approx [1, 1, 0]$, and $\Lambda \approx [1, 1, 1]$. Experimental data [3, 4] are indicated. a) $s = 1, 2$; b) $s = 1, 2, 3$ in (5)

is possible by introducing a special distortion model, referred to as "rotations", that describes rigid rotations of the neighboring quasi-ions upon a displacement of an atom [13]. However, rotations have no influence on the longitudinal modes.

3. Anisotropic Breathing

We parameterize the electron density ϱ by a set of "generalized coordinates" $\xi = \{\xi_\mu^n\}$, e.g. localization centers, decay constants, or amplitudes of the Gaussians in (5), for details see, for example [14, 15]. The displacement-induced electron-density redistribution (1) is then

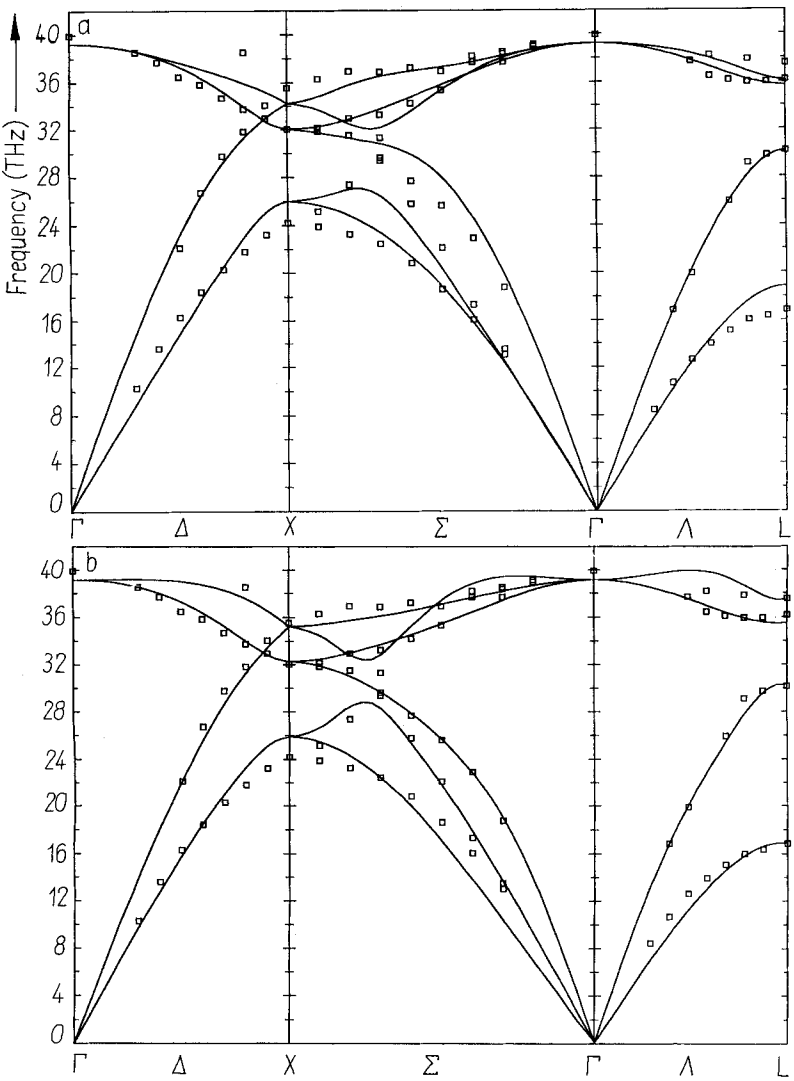

Fig. 6. Calculated phonon dispersion curves of diamond (full lines) within the rigid quasi-ion model in the main symmetry directions $\Delta \approx [1, 0, 0]$, $\Sigma \approx [1, 1, 0]$, and $\Lambda \approx [1, 1, 1]$. Experimental data [5 to 7] are indicated. a) $s = 1, 2$; b) $s = 1, 2, 3$ in (5)

given by

$$\boldsymbol{P}_{\alpha}^{m}(\boldsymbol{r}) = \frac{\partial \varrho(\boldsymbol{r})}{\partial \boldsymbol{R}_{\alpha}^{m}}\bigg|_{0} = \sum_{n,\mu} \frac{\partial \varrho(\boldsymbol{r})}{\partial \xi_{\mu}^{n}}\bigg|_{0} \frac{\partial \xi_{\mu}^{n}}{\partial \boldsymbol{R}_{\alpha}^{m}}\bigg|_{0} =: \sum_{n,\mu} f_{\mu}^{n}(\boldsymbol{r})\, \xi_{\mu\alpha}^{nm} \,. \tag{7}$$

f_{μ}^{n} is the "form factor" of the charge density variation and $\xi_{\mu\alpha}^{nm}$ describes the "reaction" of the parameter ξ_{μ}^{n} when the atom $m\alpha$ is displaced. We choose the ξ's to be localization centers of Gaussians so that

$$f_{\mu}^{n}(\boldsymbol{r}) \to \boldsymbol{f}_{\mu}^{n}(\boldsymbol{r}) = -\nabla g_{\mu}(\boldsymbol{r} - \boldsymbol{R}_{\mu}) \tag{8a}$$

with

$$g_\mu(\boldsymbol{r}) := C_\mu \left[\frac{\gamma_\mu}{\pi}\right]^{3/2} \mathrm{e}^{-\gamma_\mu r^2} . \tag{8b}$$

The index μ here comprises the four indices α, s, λ, and ν occuring in (5), i.e. $\mu = \alpha s \lambda \nu$. (Note that only the localization centers, $\boldsymbol{R}_\mu$, do actually depend on ν.) Fourier transformation leads to

$$\boldsymbol{P}_\alpha(\boldsymbol{k}) = \sum_{n,\,\mu} f_\mu(\boldsymbol{k})\, \mathrm{e}^{-i\boldsymbol{k}\cdot\boldsymbol{R}^n_{\alpha\mu}}\, \xi^{n0}_{\mu\alpha} ; \qquad \boldsymbol{R}^n_{\alpha\mu} := \boldsymbol{R}^n_\mu - \boldsymbol{R}_\alpha . \tag{9}$$

$\boldsymbol{P}_\alpha(\boldsymbol{k})$ and $f_\mu(\boldsymbol{k})$ denote the Fourier transform of $\boldsymbol{P}_\alpha(\boldsymbol{r})$ and $f_\mu(\boldsymbol{r})$, respectively, where $\boldsymbol{P}_\alpha(\boldsymbol{r})$ and $f_\mu(\boldsymbol{r})$ are defined by $\boldsymbol{P}^m_\alpha(\boldsymbol{r}) = \boldsymbol{P}_\alpha(\boldsymbol{r} - \boldsymbol{R}^m_\alpha)$ and $f^n_\mu(\boldsymbol{r}) = f_\mu(\boldsymbol{r} - \boldsymbol{R}^n_\mu)$.

Now we assume zincblende structure. We consider a Gaussian on bond ν of atom α and the corresponding Gaussian of the second atom sharing the same bond. Displacing atom $m\alpha$ leads to a displacement of both Gaussians and we find

$$\boldsymbol{P}_\alpha(\boldsymbol{k}) = \sum_{\nu,\,\lambda} \left\{ \left[f_{\alpha\lambda}(\boldsymbol{k})\, \xi^{\nu}_{\lambda}{}^{\alpha\alpha} \right] \mathrm{e}^{-i\boldsymbol{k}\cdot\boldsymbol{R}^\nu_{\alpha\lambda}} + \left[f_{\bar\alpha\lambda}(\boldsymbol{k})\, \xi^{\nu}_{\lambda}{}^{\bar\alpha\alpha} \right] \mathrm{e}^{-i\boldsymbol{k}\cdot(\boldsymbol{R}_{\alpha\nu} + \boldsymbol{R}^\nu_{\bar\alpha\lambda})} \right\} . \tag{10}$$

Since the localization type is fixed ($s = 2$) the index s has been dropped in the latter equation. $\bar\alpha$ denotes the sublattice "conjugate" to α, i.e.. $\bar 1 = 2$ and $\bar 2 = 1$. $\boldsymbol{R}_{\alpha\nu}$ are the four vectors connecting atom α with is nearest neighbors.

The tensor $\xi^{\nu}_{\lambda}{}^{\alpha\alpha}$ describes the displacement of Gaussian λ on bond ν of atom α when atom α is displaced and $\xi^{\nu}_{\lambda}{}^{\bar\alpha\alpha}$ the related displacement of Gaussian λ on bond ν of the other atom, $\bar\alpha$.

Symmetry considerations together with translational and rotational invariance lead to the final formula

$$\begin{aligned} \boldsymbol{P}_\alpha(\boldsymbol{k}) = -i \sum_{\nu,\,\lambda} \{ & [\xi_\lambda(\boldsymbol{k}\cdot\boldsymbol{R}_{\nu\alpha})\, \boldsymbol{R}_{\nu\alpha} - d_\lambda \boldsymbol{k}]\, (\mathrm{e}^{-i\boldsymbol{k}\cdot d_\lambda \boldsymbol{R}_{\nu\alpha}} - \mathrm{e}^{-i\boldsymbol{k}(1-d_\lambda)\boldsymbol{R}_{\nu\alpha}}) \\ & + \boldsymbol{k}\, \mathrm{e}^{-i\boldsymbol{k}\cdot d_\lambda \boldsymbol{R}_{\nu\alpha}} \}\, C_\lambda\, \mathrm{e}^{-k^2/(4\gamma_\lambda)} . \end{aligned} \tag{11}$$

Identical sublattices have been assumed and the sublattice index has been dropped in the case of the quantities ξ, d, C, and γ. The single independent component of the tensor $\xi^{\nu}_{\lambda}{}^{\alpha\beta}$ is described by the parameter ξ_λ. d_λ means the distance of Gaussian λ from the atom it belongs to in units of $|\boldsymbol{R}_{\nu\alpha}|$. So, per Gaussian λ, there is one free parameter ξ_λ and the rigid quasi-ion model is included via the last term in (11).

Equation (11) has a simple physical interpretation: First, the rotational-invariance requirement ensures that the Gaussians always are kept on the lines connecting nearest-neighbor atoms, even in the displaced configuration. Second, the distance of a Gaussian from the atom it belongs to is not fixed but the Gaussians may move outward or inward on the bond, depending on whether the bond is compressed or stretched. For example, the Gaussians will move outward with respect to the atom on the bonds compressed and inward on the bonds expanded if $\xi_\lambda |\boldsymbol{R}_{\nu\alpha}| - d_\lambda > 0$. This explains why we have termed this model "anisotropic breathing". Simultaneously, the Gaussian of the second atom sharing the bond will move symmetrically with respect to the bond center as a consequence of translational invariance. The model accounts for the fact that the screening charge in the middle of the bond is typically too small in the rigid-ion-model for bond-stretching-type modes (e.g.

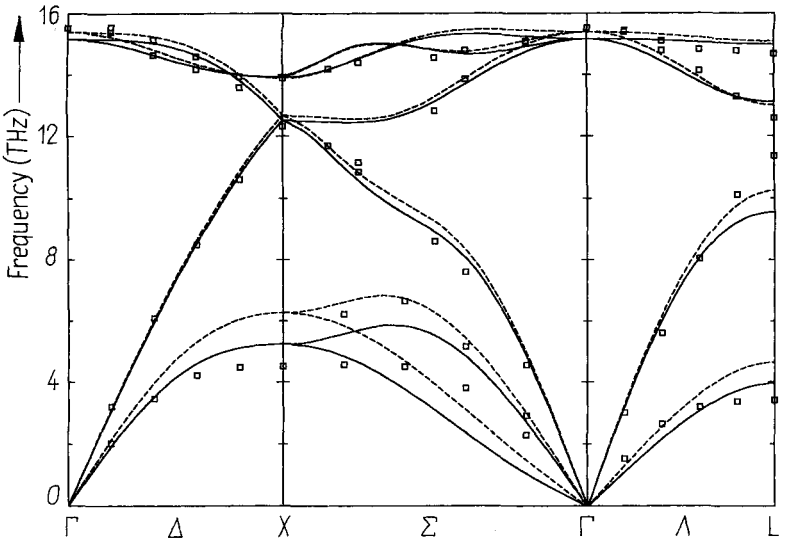

Fig. 7. Phonon dispersion curves of silicon including anisotropic breathing. Experimental data [3, 4] are indicated. $C = 0.1$, $d = -0.1$, $\xi = -1.0a^{-2}$; ——— $\gamma = 30a^{-2}$, — — — $\gamma = 80a^{-2}$

LTO(Γ) [2]), but may be increased by letting the bond-centered Gaussians move further together. This is in contrast to the *isotropic* breathing studied previously where the neighboring quasi-ion densities perform isotropic breathing motions upon the displacement of an atom.

In practice, a problem occurs when we apply (11) to the Gaussian representation (5). The different Gaussians in our representation have large positive and negative amplitudes which, however, compensate each other in the quasi-ion density and for a rigid displacement of the whole set of Gaussians. If, on the other hand, the individual Gaussians of the quasi-ion are displaced *independently*, as implied by (11), the delicate compensation gets lost and unreasonably large density changes do result. This concerns, in particular, the contribution related to the second term in the square brackets in (11) that is due to the rotational-invariance requirement. The latter term is fixed and cannot be scaled down via the parameter ξ.

Therefore, we add two new Gaussians to the representation that neutralize each other within the *rigid* quasi-ion model and include only one of the two new Gaussians in the non-rigid part of (11). So we have four parameters C, γ, d, and ξ influencing the phonon dispersion curves.

Table 1

Dependence of the LTO(Γ) and LA(L)-mode frequencies (in THz) on γ for silicon. (γ is given in units of a^{-2} where a is the lattice constant)

γ	30	40	50	60	80
LTO(Γ)	15.17	15.15	15.18	15.23	15.40
LA(L)	9.56	9.62	9.73	9.88	10.24

An example for the effects induced by such an anisotropic breathing on the phonon dispersion in case of silicon and the effect of the variation of the parameter γ is shown in Fig. 7. Substantially better dispersion curves as generated in the rigid quasi-ion model cannot be obtained. In contrast to the previously studied distortion models, the influence of anisotropic breathing does not vanish at the Γ point. Moreover, it is possible to increase

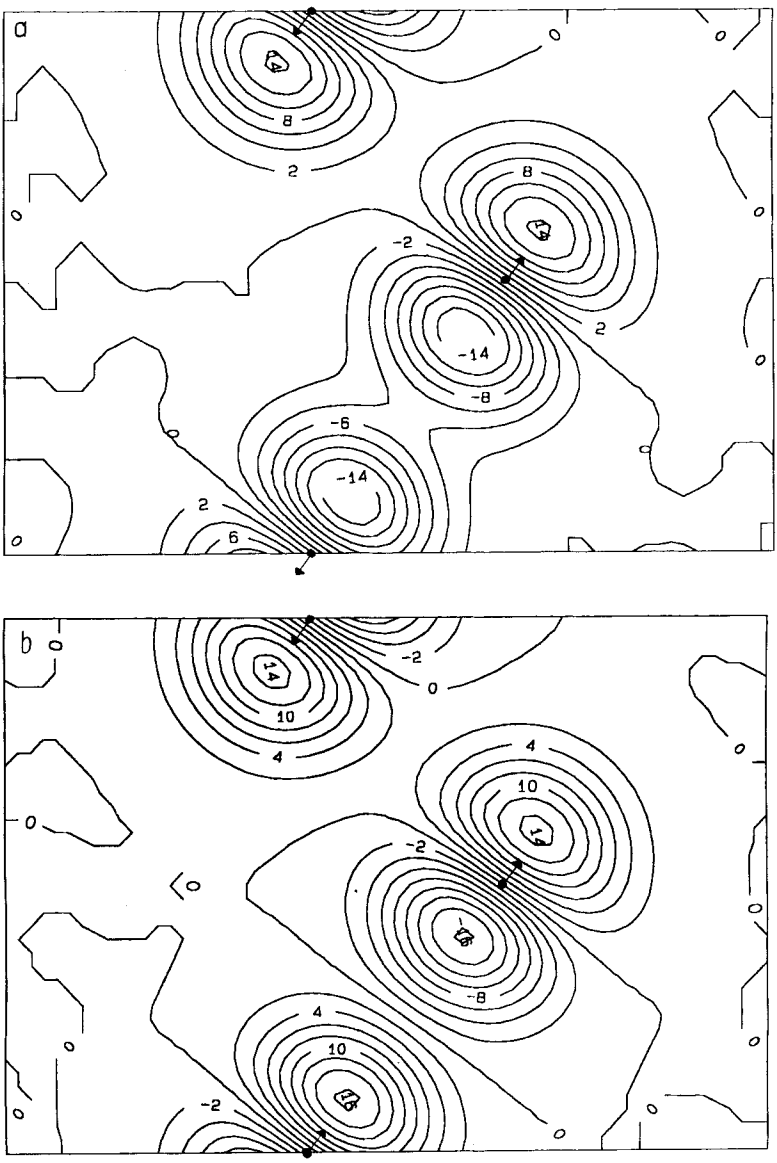

Fig. 8. Contour plot of the a) LTO(Γ)- and b) LA(L)-induced density change caused by anisotropic breathing for silicon. Units are $10\,|\boldsymbol{u}|/a\sqrt{3}$ electrons per cell and the plane is $(0, \bar{1}, 1)$. $C = 0.1, d = -0.1$, $\xi = -1.0a^{-2}, \gamma = 80a^{-2}$

the LA(L)-frequency. Depending on γ the variation of these frequencies is shown in Table 1.

Concerning the quality of the phonon dispersion curves obtained within our model one might object that it is not superior to that of other models based on a more direct parametrization of the dynamical matrix such as Weber's bond-charge model [16]. However, it should be emphasized that our main purpose here is not to achieve a perfect fit of the experimental phonon frequencies but rather to relate characteristic features in the phonon dispersion to corresponding features in the electron-density redistribution and hence get physical insight into the nature of the interatomic forces. On the other hand, it is known that the latter is not possible in the case of e.g., a simple Born-von-Karman parametrization [17].

Let us now look at the density change induced by a phonon,

$$\delta\varrho(\boldsymbol{r}) = \frac{1}{V_z} \sum_{\boldsymbol{G},\alpha} \boldsymbol{u}_\alpha \cdot [\boldsymbol{P}_\alpha(\boldsymbol{q} + \boldsymbol{G})\, \mathrm{e}^{-i\boldsymbol{G}\cdot\boldsymbol{R}_\alpha}]\, \mathrm{e}^{i(\boldsymbol{q}+\boldsymbol{G})\cdot\boldsymbol{r}}, \tag{12}$$

$\boldsymbol{u}_\alpha$ are the displacement amplitudes for the individual modes.

Because we are mainly interested in the density change caused by the anisotropic breathing alone, we exclude from (11) the Gaussians of the rigid quasi-ion model for the subsequent calculations. So the calculations presented in Fig. 8a and b have been made with one Gaussian only.

Finally, it should be mentioned that a non-vanishing quadrupole moment of the density redistribution is associated with the anisotropic breathing, in contrast to the rigid quasi-ion model where the quadrupole moment vanishes for symmetry reasons. The occurrence of a quadrupole moment in the density redistribution can easily be understood in view of the physical interpretation of the anisotropic breathing as discussed in connection with (11): The symmetric displacement of the two Gaussians on a bond leads to two oppositely directed dipoles along the bond forming together a quadrupole. It can further be shown that the quadrupoles on the four bonds, one of which is compressed, and three are stretched, do not compensate, resulting in a net quadrupole moment.

These findings are also interesting in context with the electron–phonon interaction. Calculations of, e.g., deformation potentials within the rigid quasi-ion model [18] do not contain any long-range quadrupole contributions, but in self-consistent density-functional calculations Resta et al. [19] found that a quadrupole contribution to the valence-band-edge deformation potential can be well resolved for silicon.

4. Summary

In the present paper we have investigated the phonon dispersion of diamond and silicon within the quasi-ion model. In particular, we have studied the effects of an augmentation of the expansion set for the quasi-ion densities. We find that the addition of Gaussians located on the lines connecting the next-nearest neighbors produces much better phonon dispersion curves than do Gaussians located on the bonds only. So a further addition of Gaussians seems to be useful, where up to five orders of neighbors might be taken into account for the localization. Furthermore, we have presented a model for the distortion part of the phonon-induced change in the electron density ("anisotropic breathing"). Taking into account anisotropic breathing we may, e.g., adjust the L-point longitudinal acoustic mode that is only poorly represented in the rigid quasi-ion model. In contrast to the rigid

quasi-ion model and the previously studied distortion corrections (rotations, isotropic breathing), the anisotropic breathing is associated with a quadrupole contribution to the phonon-induced density redistribution. This may be of interest in context with the electron–phonon interaction at long wavelengths.

Acknowledgement

Financial support by the Deutsche Forschungsgemeinschaft, project No. Fa 170/2-1 is gratefully acknowledged.

References

[1] C. FALTER, Physics Rep. **164**, 1 (1988).
[2] C. FALTER, M. SELMKE, W. LUDWIG, and K. KUNC, Phys. Rev. B **32**, 6518 (1985).
[3] G. DOLLING, in: Inelastic Scattering of Neutrons in Solids and Liquids, Vol. 2, IAEA, Wien 1963 (p. 37).
[4] G. NILSSON and G. NELIN, Phys. Rev. B **6**, 3777 (1972).
[5] J. L. WARREN, R. G. WENZEL, and J. L. YARNELL, see [3], Vol. 1, (p. 361).
[6] J. L. WARREN, J. L. YARNELL, G. DOLLING, and R. A. COWLEY, Phys. Rev. **158**, 805 (1967).
[7] S. SOLIN and A. K. RAMDAS, Phys. Rev. B **1**, 1687 (1970).
[8] J. R. CHELIKOWSKY and S. G. LOUIE, Phys. Rev. B **29**, 3470 (1984).
[9] M. T. YIN and M. L. COHEN, Phys. Rev. B **24**, 6121 (1981).
[10] Y. W. YANG and P. COPPENS, Solid State Commun. **15**, 1555 (1974).
[11] U. PIETSCH, V. G. TSIRELSON, and R. P. OZEROV, phys. stat. sol. (b) **137**, 441 (1986).
[12] J. A. APPELBAUM and D. R. HAMANN, Phys. Rev. B **8**, 1777 (1973).
[13] C. FALTER, W. LUDWIG, M. SELMKE, and W. E. PICKETT, J. Phys. C **20**, 501 (1987).
[14] C. FALTER, M. KLENNER, and W. LUDWIG, Physics Letters A **165**, 260 (1992).
[15] C. FALTER, M. KLENNER, and W. LUDWIG, Phys. Rev. B **47**, 5390 (1993).
[16] W. WEBER, Phys. Rev. B **15**, 4789 (1977).
[17] F. HERMAN, J. Phys. Chem. Solids **8**, 405 (1959).
[18] M. KLENNER, C. FALTER, and W. LUDWIG, Ann. Phys. (Leipzig) **1**, 24, 34 (1992).
[19] R. RESTA, L. COLOMBO, and S. SARONI, in: Phonons 89, Proc. 3rd Internat. Conf. Phonon Physics, Ed. S. HUNKLINGER, W. LUDWIG, and G. WEISS, Vol. 1, World Scientific Publ. Co., Singapore 1990 (p. 208).

(Received June 11, 1993; in revised form September 13, 1993)